

Numerical simulations of semi-armor-piercing warhead penetrating aircraft carrier target

Dong Sangqiang^{1,a}, Cai Xinghui¹, Wang Guoliang¹, Gao Yunliang¹, Lu Jiangren¹

¹ Xi'an Research Inst. of Hi-Tech in Hongqing Town, Xi'an, P.R. China

Abstract. FEM models of semi-armor-piercing warhead penetrating aircraft carrier deck are established, which are validated by related experimental data. Base on the models, the process of semi-armor-piercing warhead penetrating aircraft carrier deck with different incidence angles and attack angles are carried out. The results show that incidence angles have no remarkable influence on penetration capability of the projectile under the circumstance of zero attack angle. Ductility reaming damage mode and adiabatic plugging damage mode are exhibited in the penetration process. Attack angles have notable influence on penetration capability of the projectile. The FEM models and the results could provide reference for penetration effect research of semi-armor-piercing warhead penetrating aircraft carrier target.

1 Introduction

As an effective anti-ship weapon, semi-armor-piercing warhead has attained important application in military [1]. Numerical simulation is an important study method in high velocity impact, which needs accurate numerical models and material parameters. In this paper FEM models of semi-armor-piercing warhead penetrating aircraft carrier deck are established, which are validated by related experimental data. Base on the models, the process of semi-armor-piercing warhead penetrating aircraft carrier deck with different incidence angles and attack angles are carried out.

2 Modeling and Validating

2.1 Grid Model

A half grid model of the projectile and the target are established as Fig.1 and Fig.2 showed. The projectile is made up of shell, charge and fuze, which is 16kg in weight, 370mm in length, and 105mm in diameter. The projectile has a truncated oval nose with diameter of 20mm.



Figure 1. FEM model of the projectile.



Figure 2. FEM model of the target.

The simplified grid model of the target about “Nimitz-class” aircraft carrier with deck thickness of 50mm is created according to the literature [1]. A non-reflection boundary condition is defined to simulate large extent in length.

2.2 Material models

According to relative literatures [2, 3], materials of the shell and the target are 30CrMnSi and 921A respectively, and the home-produced 9211A is equivalent to HY-80 in mechanical performance which is used in the carrier of the U.S. In this numerical simulation model, plastic kinetics model is adopted to describe mechanics behavior of the shell and the target, which considers the effect of strain rate by Cowper-Symonds model,

$$Y = \left[1 + \left(\frac{\dot{\epsilon}}{C} \right)^{1/p} \right] (\sigma_0 + \beta \epsilon_{eff})$$

Where, Y is yield stress, $\dot{\epsilon}$ is strain rate, ϵ_{eff} is effective plastic strain, σ_0 is yield stress in static state, C and p are material constants, β is strength factor, $0 \leq \beta \leq 1$.

^a Corresponding author: shinedsq@126.com

The parameters in the model are evaluated according to literatures [2-5], which are listed in Table 1 and Table 2.

Table 1. Parameters of the shell[2-5].

$\rho /(\text{kg}/\text{m}^3)$	$E /(\text{GPa})$	ν	σ_0 / MPa
7.85	210	0.28	1600
$ET /(\text{GPa})$	C	P	ϵ_{eff}
2.1	1.0	100	1.8

Table 2. Parameters of the target [2-5].

$\rho /(\text{kg}/\text{m}^3)$	$E /(\text{GPa})$	ν	σ_0 / MPa
7.8	205	0.3	685
$ET /(\text{GPa})$	C	P	ϵ_{eff}
0.19	1.0	100	1.6

The other parts in the projectile are treated as elastic materials, of which the density of the charge and the fuze are $1.7\text{g}/\text{cm}^3$ and $3.8\text{g}/\text{cm}^3$ respectively.

2.3 Model validation

According to relative literatures [6-8], an FEM validation model is established as shown in Fig.3 and Fig.4, in which the projectile and material models are same with ones described above, and the target is ribbing-stiffened and homogeneous with multi-layered space structure.

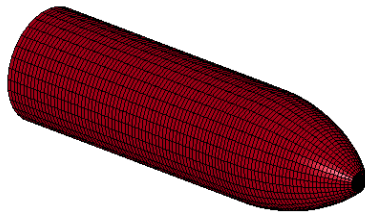


Figure 3. FEM validation model of the target.

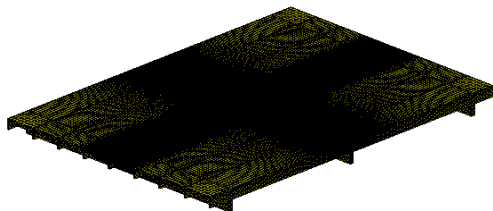


Figure 4. FEM validation model of the target.

With the model, three-dimensionally numerical simulations are carried out by LS-DYNA to analyze nine instances of the projectile impacting the target with different incidence angles. The results show that maximal errors and average errors of calculated values of residual

velocity relative to experimental results described in literatures [6] are respectively 6.81% and 2.37% for all the nine cases. And that deck damage effects obtained by numerical simulation are in accord with ones in related experiments. The FEM models constructed above are valid and could provide reference for penetration effect research of semi-armor-piercing warhead penetrating aircraft carrier target.

3 Influence of incidence angles

3.1 Penetration capacity

With the model constructed above, three-dimensionally numerical simulations are carried out by LS-DYNA to analyze six instances of the projectile impacting the target with different incidence angles of 0° , 5° , 10° , 15° , 20° , 25° and the same attack angle of 0° . In all the six instances, the initial impact velocity of the projectile is same as $600\text{m}/\text{s}$. The time history curves of velocity and acceleration of the projectile in all six instances are given in Fig.5 and Fig.6 respectively.

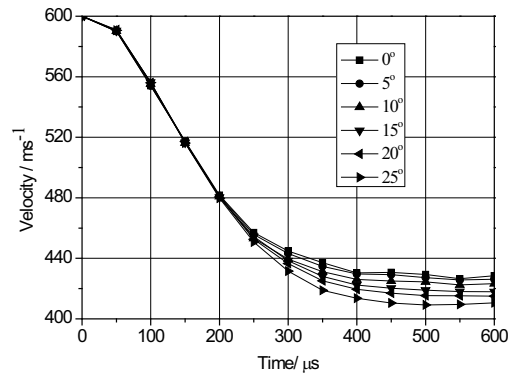


Figure 5. History curves of velocity.

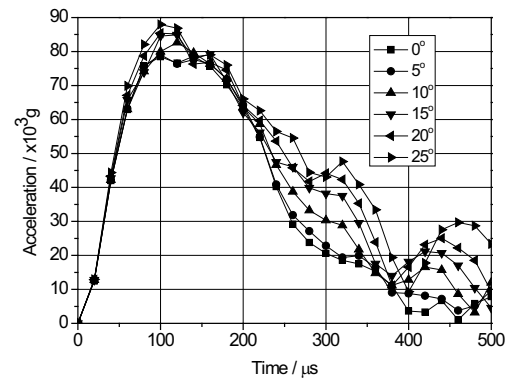


Figure 6. History curves of acceleration.

As shown in Fig.5 and Fig.6, incidence angles have no remarkable influence on residual velocity and maximal acceleration of the projectile under the circumstance of zero attack angles. In all six instances, the values of residual velocity of the projectile are $429\text{m}/\text{s}$, $426\text{m}/\text{s}$, $423\text{m}/\text{s}$, $417\text{m}/\text{s}$, $415\text{m}/\text{s}$ and $411\text{m}/\text{s}$

respectively, and the values of maximal acceleration of the projectile are 78644g, 79072g, 82664g, 84925g, 85408g and 87980g respectively. In the case of the incidence angle of 25°, it is an appreciable decrease of 4.2% in residual velocity and an appreciable increase of 11.9% in maximal acceleration compared with the case of the incidence angle of 0°. It can be concluded that incidence angles have no remarkable influence on penetration capability of the projectile under the circumstance of zero attack angles, which are mainly contributed by varying in penetration process which increases with the incidence angle.

3.2 Damage conformation

Dynamic response moment of the target and projectile in three instances are given in fig. 5. As shown in Fig.7, the nose of the projectile suffers from serious erosion process as a result of its truncated oval shape and violent interaction with the target, while in whole penetration process of all the six instances the overall structure of the projectile could keep intact with no evident deformation.

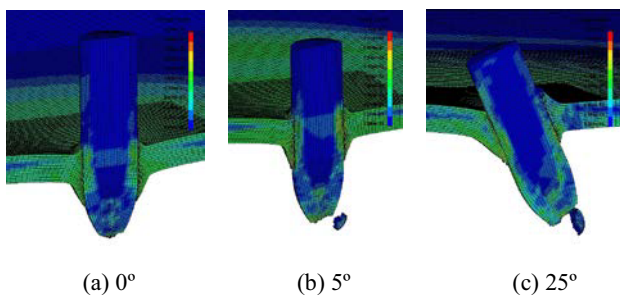


Figure 7. Dynamic responses of the target.

For the target, ductility reaming damage mode is exhibited in the penetration processes of all the instances. Furthermore when the attack angle is larger than 5°, adiabatic plugging damage mode is exhibited with different size of plugs formed in all other instances, which could be contributed by interaction of compression wave and dilatational wave at the back of the target.

4 Influence of attack angles

4.1 Penetration capacity

With the FEM established in the paper, three-dimensionally numerical simulations are carried out to analyze twelve instances of the projectile impacting the target with six different attack angles, namely 0°, 5°, 10°, 15°, 20° and 25°, respectively under the conditions of incidence angle of 0° and 25°. In all the instances the initial velocity of the projectile is 600m/s.

When the incidence angle is 0°, as shown in Fig.8, some change in attack angles has notable influence on penetration capability of the projectile. When the attack angle are 5°, 10°, 15°, 20°, and 25°, the values of residual velocity of the projectile decrease 1.7%, 7.4%, 17.8%,

34.6%, and 54.5% respectively relative to the one in attack angle of zero. The residual velocity is 192m/s when the attack angle is 25°.

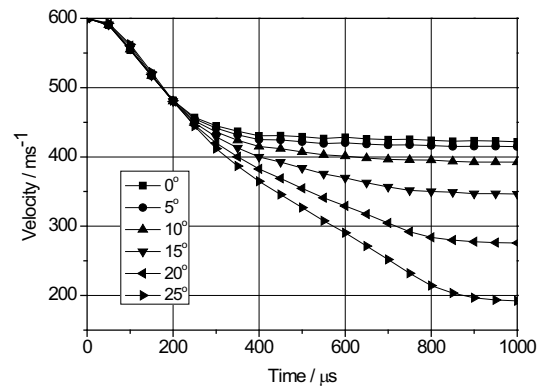


Figure 8. History curves of velocity (incidence angle of 0°).

When the incidence angle is 25°, as shown in Fig.9, some change in attack angles has similar influence on penetration capability of the projectile with the case of incidence angle of 0°. When the attack angle are 5°, 10°, 15°, 20°, and 25°, the values of residual velocity of the projectile decrease 1.5%, 7.3%, 14.9%, 27.3%, and 42% respectively relative to the one in attack angle of zero. As listed in Table 3 and Table 4, when the attack angle is larger than 15°, the residual velocity has an obvious increase compared with the case of incidence angle of 0°.

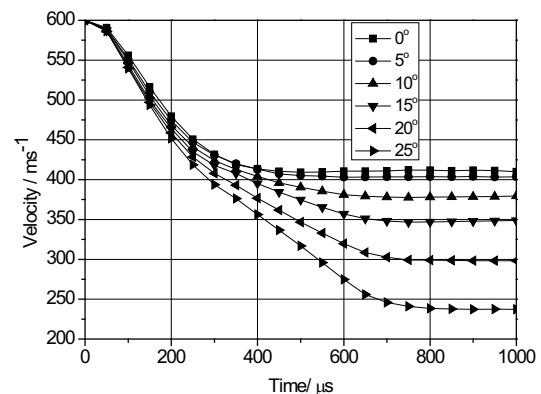


Figure 9. History curves of velocity (incidence angle of 25°).

Table 3. The results of incidence angle of 0°.

Attack angle	residual velocity /(m/s)	Acceleration /(g)
0°	422	78644
5°	415	79929
10°	393	81504
15°	347	81396
20°	276	83308
25°	192	87683

Table 4. The results of incidence angle of 25°.

Attack angle	residual velocity / (m/s)	Acceleration / (g)
0°	410	87980
5°	404	90131
10°	380	97817
15°	349	100979
20°	298	104197
25°	237	107308

As showed in Fig.10, when the incidence-angle is 0°, change in attack angles has no obvious influence on the maximal accelerations. When the attack angle is 25°, the value of maximal accelerations achieved 87683g, which has an increase of 11.5% relatively to the one in zero attack angle. While compared with the instance of zero attack-angle, durative high accelerations come forth in the penetration process of other five instances, which maybe lead to serious problems in structure integrity and charge stability.

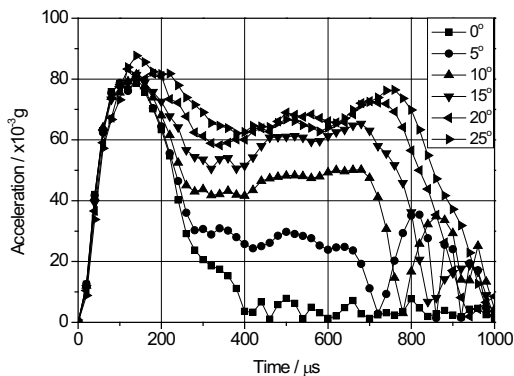


Figure 10. Acceleration curves (incidence angle of 0°).

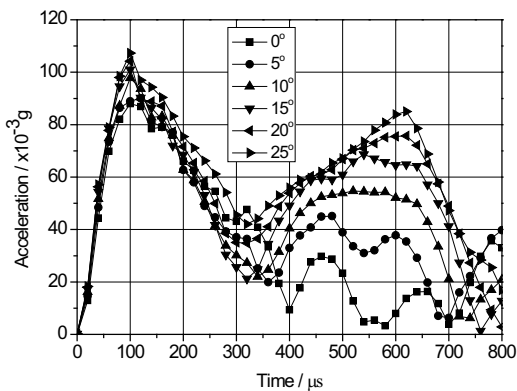


Figure 11. Acceleration curves (incidence angle of 25°).

But when the incidence angel is 25° showed in Fig.11, change in attack angles has evident influence on the maximal accelerations. When the attack angle is 25°, the value of maximal accelerations achieved 107308g,

which has an increase of 22.0% relatively to the one in zero attack angle. Furthermore as listed in table 3, for the two different incidence angles, the incidence angel has obvious influence on the maximal accelerations. For the case of 20° attack angle and 25° incidence angle the maximal acceleration has a maximal increase of 25.1% compared with the case of 20° attack angle and 0° incidence angle, which can be concluded that when the incidence-angle is 0° or the attack-angle is 0°, change to some extent of landing posture of the projectile has no obvious influence on the maximal accelerations, but when attack angle and incidence angle both change to some extent, the influence is appreciable.

4.2 Damage conformation

Dynamic responses moment of the target and projectile in three instances are given in Fig.12 and Fig.13. Penetration course of the projectile with attack angle of 25° is given in Fig.14.

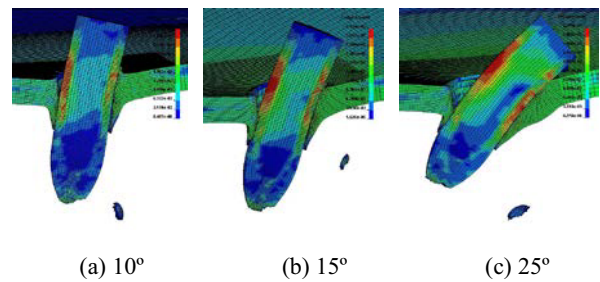


Figure 12. Dynamic responses (0° incidence angle).

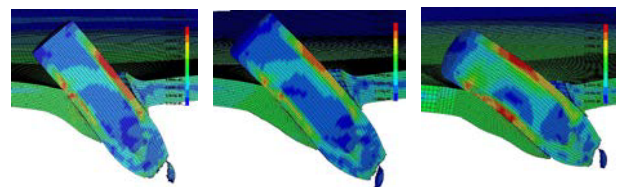


Figure 13. Dynamic responses (25° incidence angle).

As shown in Fig.12 and Fig.13, the nose of the projectile suffers from serious erosion process as a result of its truncated oval shape and violent interaction with the target. For the target, ductility reaming damage mode is exhibited in the penetration processes of all the instances. Furthermore when the attack angle is larger than 10°, adiabatic plugging damage mode is exhibited with different size of plugs formed at the back of the target in all other instances.

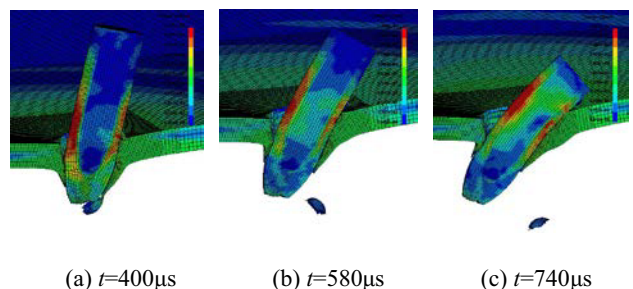


Figure 14. Penetration course of the projectile (25° attack-angle and 0° incidence-angle).

As shown in Fig.14, when the attack angle is equal to 0° , the overall structure of the projectile could keep intact with no evident deformation. While when the attack angle is larger than 5° , the projectile suffer from varying degrees of structure distortion as results of moment loading caused by forces from lateral action, and the structure distortion become serious in extent with increasing of the attack angle. Furthermore, as shown in Fig.5, structure distortion of the projectile suffer from a process of first bending left and subsequently turn right, which could lead to serious risk for the integrity of the projectile structure and the stability of the charge.

5 Conclusions

(1) FEM models of semi-armor-piercing warhead penetrating aircraft carrier deck are established by numerical simulation method, which are validated by related experimental data.

(2) Change in attack angles has notable influence on penetration capability of the projectile. When the attack angel are 5° , 10° , 15° , 20° , and 25° , the values of residual velocity of the projectile decrease 1.7%, 6.9%, 17.8%, 34.6%, and 54.5% respectively relative to the one in attack angle of zero. Change to some extent in attack-angle or incidence-angle has no obvious influence on the maximal accelerations, but when attack angle and incidence angle both change to some extent, the influence is appreciable.

(3) The projectile suffer from varying degrees of structure distortion when the attack angle is larger than 5° and the structure distortion become serious in extent with increasing of the attack angle. For the case discussed in this paper, it is suitable for the projectile to keep an attack angle of no more than 10° .

References

1. Lan Ling. Torpedo Technology. **10**, 8(2002)
2. Jones N. Structural Impact [M]. (1st Edition, 1989). Paperback Edition Cambridge, Cambridge University Press, 403(1977)
3. LS-DYNA KEYWORD USER'S MANUAL[CP]. March 2003 Version 970
4. Zhang Lin, Zhang Zugen, QIN Xiaoyun, etc. Chinese Journal of High Pressure Physic. **17**,305(2003)
5. Liu Xinde. Aerospace Materials and Technology. 29(1985)
6. Duan Zhuoping. Explosion and Shock Waves. **25**,547(2005)
7. Duan Zhuoping, Zhang Zhongguo, Li Jingzhu, etc. Journal of Projectiles, Rockets, Missiles and Guidance. **25**,148(2005)
8. Song Weidong, Ning Jianguo, Zhang Zhongguo, etc. Journal of Ballistics. **16**,49(2004)